



A NEW HYBRID APPROACH BASED ON PROBABILITY DISTRIBUTION AND AN IMPROVED MACHINE LEARNING FOR MULTIVARIATE RISK ASSESSMENT

Abdelhakim AZZEDINE ^{1,*} , Fatma Zohra NOURI ¹ , Salah BOUHOUCHE ²

¹ Mathematical Modeling and Numerical Simulation Research Laboratory, Faculty of Sciences, Badji Mokhtar University, BP12, Annaba, Algeria.

² Research development, innovation and Technological Support Bureau - BRD InovScience. Adresse: UV12, Bloc09 Bureau 17BIS Industrial Group SIDER, S/Amar Annaba Algeria.

* Corresponding author, e-mail: azzedine.abdelhakim@gmail.com

Abstract

A highly complex dynamic non-linear reactor is the blast furnace iron manufacturing system. It has possible dangers, including carbon monoxide, wide variety of chemical reactions, fire, high pressure and explosion, noise, split and fall, hot metal sparks, hit etc. To ensure a secure working, organizations must take the required measures to manage the risks and their effects. The approach for risk assessment discussed in this research attempts to increase blast furnace safety performance and reduce workers injuries. This approach uses probability distribution and an improved machine learning techniques such as radial basis function artificial neural networks (RBANN). The novelty here is to calculate a multivariate risk using a proposed method, namely exponential smoothing combined with radial basis function artificial neural networks (ES-RBANN). To identify their limits, the results of a research comparing conventional and novel techniques are confirmed using real data collected from the steel production operations ArcelorMittal-Annaba, Algeria.

Keywords: blast furnace; exponential smoothing; risk and safety; data driven techniques; probability distribution

List of Symbols/Acronyms

λ_{t-1} – Constant at t-1 time;
 H_{t-1} – Hessian matrix;
 e_{t-1} – Modeling error;
 $y_{pn,t+1}$ – Output of ES-RBANN technique at t+1 time;
 ε – Error;
 b_l – Bias l^{th} in the output layer;
 I – Identity matrix;
 $y_{c,t}$ – Output calculated by the probability distribution at t time;
 w_{lk} – Weight between the k^{th} neuron in the hidden layer and the l^{th} neuron in the output layer;
 J_{t-1} – Jacobian matrix;
 $y_{p,t+1}$ – Output of RBANN technique;
 \hat{y}_l – Predicted output of the node network output layer;
 T_L – Single lower tolerance limit;
 T_U – Single upper tolerance limit;
 $\|\cdot\|$ – Euclidean norm;
 c_k – Center;
 ES-RBANN – Exponential smoothing combined with radial basis function artificial neural networks;
 G_k – k activation function;
 P_c – Conformity probability;
 PDF – Probability density function;
 $R(t)$ – Reliability function;
 RBANN – Radial basis function artificial neural networks;
 U – Standard uncertainty;

x – Input variables;
 Z – Standardization;
 γ – Width of the hidden layer;
 μ – Mean;
 σ – Standard deviation;
 φ – Cumulative density function CDF;
 α – Regularization parameter;

1. INTRODUCTION

The Modern manufacturing systems often consist of a number of dependent parameters that have been identified, as it is difficult to analyze and monitor. The stable and safe operation of each process is critical to the success of the system; however, deviations from the norm reduce productivity. Therefore, regular monitoring is necessary to preserve the production's performance and quality. As a result of continuous monitoring, estimating the evolution of the risks and failures becomes possible to predict precaution and maintenance policies. Analyzing product quality can be challenging because of the uncertainty in time delay needed to obtain accurate findings, especially in complex systems such as blast furnace.

Blast furnace ironmaking is a major source and an essential part of both iron and steel

manufacturing. They are expensive assets that have a significant contribution to lifting a country's economy, and any accidents or malfunctions can lead to significant financial losses. Risk assessment helps protect these valuable assets and emergency preparedness. Safety is a major issue, and knowing the hazards related to their operation is crucial to protect workers and the surrounding environment, including air and water. For this, we are willing to develop new techniques to improve safety practices. The pig iron temperature, circular pressure, and hot wind temperature are the most important indicators of blast furnace production and hazard; so by only predicting the multivariate risk of those parameters can approximately control blast furnace process. Nowadays there are many ways for blast furnace risk assessment research, we can cite failure modes and effects analysis (FMEA) [17], ultrafine particle risk assessment in the blast furnace production process [7], hazardous amounts of cement based solidification process are produced when fly ash and blast furnace slag from municipal solid waste incinerators are combined [12], forecast of blast furnace gas production using data driven and mechanism techniques [11] and [16] and modeling and identifying metallurgical systems using multivariate statistical control and data mining techniques [7, 8, 10, 19].

Generally, the different hazard is evaluated using the above-cited methods like FMEA. In this paper, we propose a novel method for measuring and monitoring blast furnace quality and analyze a multivariate risks using hybrid dynamic method based on a robust artificial intelligence method and probability distribution.

The major motivations using this approach are:

1. The application nature is characterized by a multivariate and highly nonlinear system.
2. The proposed approach is quite easy to implement.

This paper is structured as follows: The suggested inferential model for risk assessment is presented in Section 2, utilizing data mining and the normal probability distribution. With credible data, Section 3 provides a typical application of how the suggested procedures are used; where the first step is to assess the local (upper/lower) and global risks based on probability theory, and the second one is modelling. At this latter, multiple regression models are developed using the calculated risks in the first step, taking into account all dependencies. We finish with a comparative study between conventional and developed methods, and concluding remarks.

2. BLAST FURNACE IRONMAKING SYSTEM WITH OPTIMIZATION TECHNOLOGY

Blast furnace is one of the most important industrial processes using coal and coke as primary fuel, its main components are several specific such as charging equipment; cooling circuit, hot wind

production assembly, and large cylindrical shaft furnace.

The temperature of hot metal and pressure in the ironmaking industry does not only signify the consumption of energy but also reflects the degree of purity and manufacturing rate. When the temperature rises too high, a great amount of fuel is consumed, and breakages can occur, resulting significant increases in productivity losses and maintenance expenses. Conversely, if the temperature gets too insufficient, the blast furnace tap holes can get clogged, and production costs for following steelmaking processes will rise [19]. Additionally, inadequate pressure can slow down the combustion of coke and impedes the chemical reactions necessary for the reduction of iron ore, leading to lower production rates and a reduced overall efficiency.

Their main operation mode is as follows: from the top of the furnace, successive layers of solid raw materials like ore iron and coke are charged [11]. Due to their unique weight, they progressively sink to the bottom of the heating until it melts. Whereas, the hot combustion gases ascend via the combustion column materials. These combustion and gasification events generate a tremendous quantity of heat, resulting in a high flame temperature in the raceway zone ranging from 1231 °C to 1478 °C [19]. As the molten metal flows, it combines with cast iron and slag upon entering the crucible. At the point of combustion, the materials separate in two parts: molten slag on one aspect and molten hot metal (typically contains about 92-94% iron). On the opposite aspect, those accumulate in accordance to its respective specific masses. The slag pouring hole, that is set higher than the cast iron pouring hole, is used to evacuate the slag. After a long time of 6-8 hours, the adjusted factors from the top (pig iron and coke) transform the hot metal compositions. The adjusted factors (gas, hot and air) entering from the bottom have an attractive immediate influence on the compositions. In most cases, the composition of both the hot metal and the slag is determined through spectroscopic measurements conducted on samples from these materials. Blast furnace slag is widely used in industry for binders, artificial stone, thermal insulation materials (slag pumice and slag wool) and slag cement. Furthermore, it can be used as an aggregate in road construction and maintenance. On the other hand, hot metal can be alloyed with other metals to create specific alloy compositions with desirable properties. Modeling blast furnaces is quite challenging because of the high pressure, diverse chemical reactions, and complicated heat and mass transmission mechanisms that occur between multi-phase materials, such as solid-solid, solid-gas, liquid-liquid and liquid-gas phases interacting [20]. Despite the finest expert attempts to resolve these issues, difficulties still exist (see Diagram 1). Our motivation is to explore the capability of both conventional and advanced methods to build credible models capable of accurately forecasting

Pig iron temperature risk. This parameter possesses a significant importance as it plays a crucial role in estimating the quality of iron in the blast furnace process.

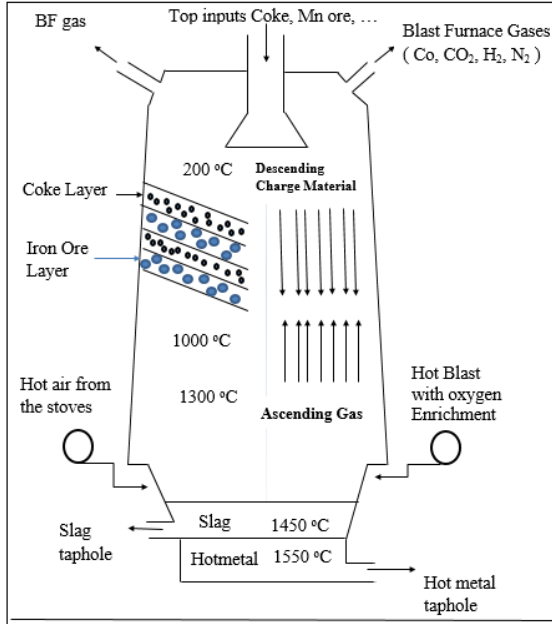


Diagram 1. A schematic of the blast furnace.

3. RELIABILITY ASSESSMENT AND DATA DRIVEN TECHNIQUES

3.1. Normal Distribution

In many research fields such as statistics and data analysis, the normal distribution, often known as the Gaussian distribution or bell curve, is one of the most popular and important continuous probability distributions [10,14]. The probability density function (PDF) for the normal distribution is defined as follows:

$$f(t) = \frac{1}{\sqrt{2\pi}\sigma} e^{-\frac{1}{2}\left(\frac{t-\mu}{\sigma}\right)^2}, (-\infty \leq t \leq +\infty) \quad (1)$$

Where μ and σ are the distribution parameters (μ = mean, σ = standard deviation), and the cumulative density function (CDF) for the normal distribution is given by:

$$F(t) = \int_{-\infty}^t \frac{1}{\sqrt{2\pi}\sigma} e^{-\frac{1}{2}\left(\frac{t-\mu}{\sigma}\right)^2} dt \quad (2)$$

The reliability function $R(t)$ for normal distribution is defined by:

$$R(t) = \int_t^{+\infty} \frac{1}{\sqrt{2\pi}\sigma} e^{-\frac{1}{2}\left(\frac{t-\mu}{\sigma}\right)^2} dt \quad (3)$$

The Z transformation used to transform the normal PDF to the so-called standard normal PDF, for which $\mu = 0$ and $\sigma = 1$, is of the form:

$$z = \frac{t - \mu}{\sigma} \quad (4)$$

to give the so-called cumulative density function

$$\varphi(z) = \int_{-\infty}^z \frac{1}{\sqrt{2\pi}} e^{-\frac{z^2}{2}} dz \quad (5)$$

3.2. Conformity probability and associated risk levels

To assess the conformity of specified parameters, several items are required, such as an interval $[T_L, T_U]$ of allowed values of the parameters is provided, where T_L and T_U are single lower and upper tolerance limit, respectively, as shown in Diagram 2.. Additionally, the ability to measure the property and express the measurement results in according to the Guide Uncertainty Measurement's principles [4 and 14].

The probability that measures x in the given range $[m, n]$ (m, n are taken from the data) is

$$P(m \leq x \leq n) = \int_m^n f(t) dt = F(n) - F(m), \quad (6)$$

where x represents the input variables, which include Pig iron temperature, Circular pressure, and Hot wind temperature.

Using the procedure that led to expression (6), the probability for $m \leq x \leq n$

$$P(m \leq x \leq n) = \varphi\left(\frac{n-x}{u}\right) \varphi\left(\frac{m-x}{u}\right), \quad (7)$$

where u is the standard uncertainty.

A. One-sided tolerance intervals with normal PDFs

*Single lower tolerance limit

From expression (7), with $m = T_L$, $n \rightarrow \infty$ and note that $\varphi(\infty) = 1$, the conformity probability is:

$$p_c = 1 - \varphi\left(\frac{T_L - x}{u}\right) \quad (8)$$

As $\varphi(t) + \varphi(-t) = 1$, equation (8) can be expressed as follow:

$$p_c = \varphi\left(\frac{x - T_L}{u}\right) \quad (9)$$

*Single upper tolerance limit

The conformance probability is as follow using equation (7), with $m \rightarrow \infty$, $n = T_U$, and note that $\varphi(-\infty) = 0$:

$$p_c = \varphi\left(\frac{T_U - x}{u}\right) \quad (10)$$

B. Two-sided tolerance intervals with normal PDFs

Equation (7) with $n = T_U$ and $m = T_L$ leads to the conformance probability:

$$p_c = \varphi\left(\frac{T_U - x}{u}\right) - \varphi\left(\frac{T_L - x}{u}\right) \quad (11)$$

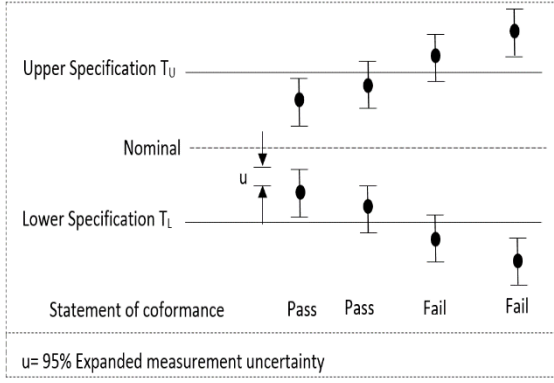


Diagram 2. Interval of tolerance with a Two-sided tolerance limit

3.3. Radial Basis Function Artificial Neural Network (RBANN)

The RBANN is a universal non-linear layered, special type of feed-forward supervised neural networks, typically is consisting of three layers namely input, output, and just one hidden layer composed of a number of RBANN non-linear activation units or more. Activation functions in RBANN are ordinarily defined as Gaussian functions. Moreover, RBANN benefit from important advantages such as the accuracy, the robustness, and the faster learning speed. For more details, refer to ([6] and [18]).

The network hidden layer output of the k^{th} activation function G_k is calculated using the following equation:

$$G_k(\|x - c_k\|) = e^{-\frac{\|x - c_k\|^2}{\gamma^2}} \quad (12)$$

Here, $\| \cdot \|$ is the Euclidean norm, c_k is the center, and γ is the width of the hidden layer.

In this case, the output \hat{y}_l of the node l of the Network output layer can be computed by:

$$\hat{y}_l = \sum_{k=1}^n w_{lk} G_k + b_l, \quad (13)$$

Where w_{lk} is the weight between the k^{th} neuron in the hidden layer and the l^{th} neuron in the output one, and b_l is the l^{th} bias in the output layer.

The identified model using RBANN is estimated by a robust algorithm, such as Levenberg-Marquardt. The following formula provides the recursive form:

$$W_{kl}^t = W_{kl}^{t-1} - (H_{t-1} + \lambda_{t-1} I)^{-1} J_{t-1}^T e_{t-1} \quad (14)$$

where I is the identity matrix with λ_{t-1} a constant and e_{t-1} , H_{t-1} and J_{t-1} are the modeling error, the Hessian and the Jacobian, respectively.

The general structure of RBANN network applied in this work is defined as follow:

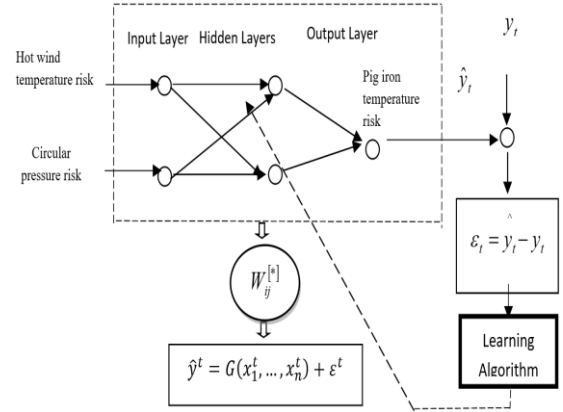


Diagram 3. Structure of RBANN network.

3.4 Exponential Smoothing combined with RBANN (ES-RBANN)

For the Exponential Smoothing method, we refer to [1] with the following equations:

$$\varepsilon_{t-1} = y_{c,t-1} - y_{p,t-1}, \quad (15)$$

$$\varepsilon_t = y_{c,t} - y_{p,t} \quad (16)$$

Here we try to compute the first smoothing value y_{pn} and the parameter α

$$\varepsilon_{t+1} = \alpha * \varepsilon_t + (1 - \alpha) * \varepsilon_{t-1} \quad (17)$$

$$y_{pn,t+1} = y_{p,t+1} + \varepsilon_{t+1} \quad (18)$$

where ε is error, $y_{c,t}$ is the output calculated by the probability theory at time t . $y_{p,t+1}$ and $y_{pn,t+1}$ are the output of RBANN and ES-RBANN techniques at time $t + 1$, respectively.

4. MULTIVARIATE RELIABILITY ANALYSIS APPLICATION IN BLAST FURNACE

In this section, we present the risk evaluation model structure, as shown in Diagrams 4 and 5.

Note that the inputs of RBANN are Hot wind temperature and Circular pressure risks, while the output is Pig iron temperature risk.

The graphical representation of input models are shown in Figure 1. Tables 1. and 2. show the descriptive statistics of collected samples and the Correlation Matrix, respectively.

Additive risk: is an addition operation of the defect probability of different causes, this is applied if at least one cause could generate a defect,

Multiplicative risk: is a multiplication operation of the defect probability of different causes, this is applied if all causes could generate a defect,

Global risk: is a combine relationship between additive and/or multiplicative risks.

4.1. Numerical experimentation

The developed numerical algorithms and the obtained results for the method described in the previous sections are presented in this section.

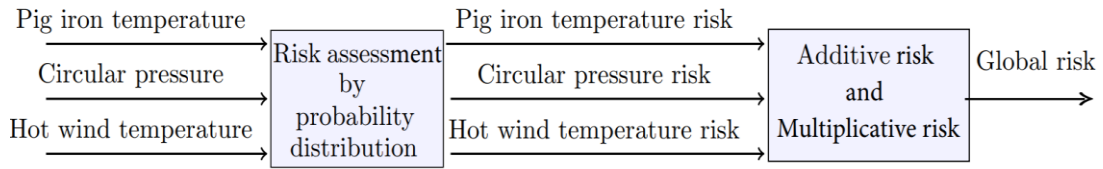


Diagram 4. Model structure using probability theory

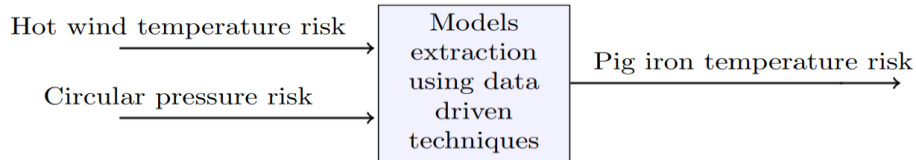


Diagram 5. Model structure using data driven techniques

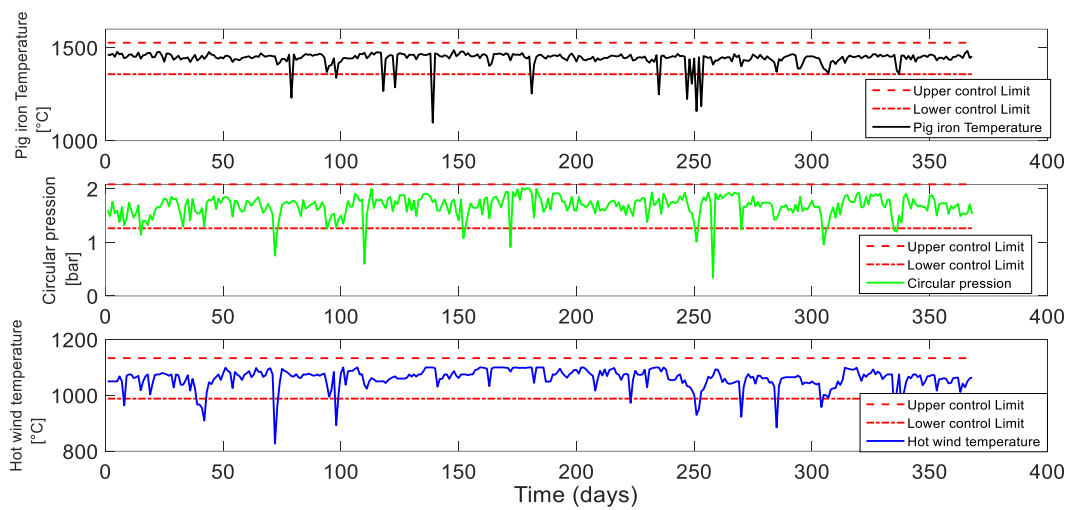


Fig. 1. The graphical representation of model inputs

Table 1. Descriptive statistics of collected samples

Descriptive statistics	Parameters		
	Pig iron temperature	Circular pressure	Hot wind temperature
Mean	1446.50	1.6	1055.20
Median	1451	1.66	1070
Mode	1443	1.54	1075
STD Deviation	29.04	0.24	43.69
Variance	843.45	0.059	1909.03
Coefficient of variation	2.93	12.26	3.41
Range	247	1.91	273
Minimum	1231	0	827
Maximum	1478	1.91	1100

Table 2. Correlation Matrix

	Pig iron Temperature	Circular Pressure	Hot wind Temperature
Pig iron temperature	1	0.1173	0.2453
Circular pressure	0.1173	1	0.4675
Hot wind temperature	0.2453	0.4675	1

Risk evaluation using probability theory

Algorithm

Step 1: Define upper control limit T_U .

Step 2: Define Lower control limit T_L .

For $i = 1 : N$ (N = Number of inputs)

For $j = 1 : M$ (M = Number of samples)

Step 1: Normalization using equation (4).

Step 2: Compute normal probability distribution.

Step 3: Compute conformance probability of lower and upper tolerance limit using (9) and (10), respectively.

Step 4: Compute conformance probability of Two-sided using equation (11).

end j,

end i.

RBANN Algorithm

The developed RBANN algorithm in the multivariable form is implemented using the following Algorithm.

Step1: Initialize the network weights as :

$f \rightarrow RBANN$.

Step2: Initialize the network weights to be:

$W_{ij}^0 = [-0.5, +0.5]$.

Step3: The computational loop is characterized as for $t = 1 : M$,

1. Acquisition of inputs/outputs (x^t, y^t) .

2. Compute G using equation (12).

3. Calculate the output model $\hat{y}(t)$ from (13).

4. Calculate the modeling error $e(t) = y(t) - \hat{y}(t)$

a) If $e(t) \approx 0$, $W_{ij}^t = W_{ij}^{t-1}$ stop: $W_{ij}^t = W_{ij}^{[*]}$.

b) Else, use the recursive algorithm to adjust the NN weights:

$W_{ij}^t = W_{ij}^{t-1} + G(t)e(t)$ by Levenberg-Marquardt algorithm from equation (14).

End t.

ES-RBANN Algorithm

we use the same procedure as in RBANN algorithm together with the following loop

For $i = 1 : M$,

Step1: Compute the residual at times $t-2$ and $t-1$ from equations (15) and (16).

Step2: Compute the residual at time t using equation (17).

Step3: Compute the first smoothing value y_{pn} using equation (18).

End i,

Step4: Compute Standard deviation uncertainty between the output model and the prediction.

4.2. Results and Discussion

The present risk assessment study was proceeded as follows:

- First, the different risks of exceeding limits were evaluated by using theory of probabilities and assuming that the distribution laws are normal for each parameter,
- As the process is complex, it contains several parameters, so the first step is completed by the

search of complex relationship between various generated risks and the final situation i.e. the global risk,

- Additive or multiplicative risks are introduced to generate the global risk according to the process type (parallel or series) i.e. a risk can be a result of combination of other risks according to the system complexity.

In order to improve training and testing phases, a modest number of samples of 365 tests and several input variables have been used for this study. Finally, a comparative study between RBANN and ES-RBANN techniques is realized, and the best model is selected using standard deviation (STD) performance indicator.

The obtained results are resumed in Tables 1-5 and Figures 1-5, such that:

Figure 1 represents results for the three variables, Pig iron temperature, Circular pressure, Hot wind temperature as a function of time in days, along with their upper and lower control limits.

Table 1 gives us the different statistical summary of collected data. These statistics provide insights into the central tendency (Mean, Median, and Mode), variability (Range, Variance, Standard deviation, and Coefficient of variation), and distribution (Skewness and Kurtosis) of data for each of the three variables. These results can be helpful for further analysis and decision-making related to the dataset.

Table 2 shows that the Circular pressure exhibits a moderate positive correlation with Hot wind temperature, with a correlation coefficient of around 0.4675; while, the correlation between Pig iron temperature and Circular pressure is approximately 0.1173, indicating a relatively weak positive correlation. This means that as Pig iron temperature increases, there is a slight tendency for Circular pressure to increase as well. At last, the correlation between Pig iron temperature and Hot wind temperature is about 0.2453, showing a moderately positive relationship. When the temperature of the pig iron raises, the temperature of the hot wind also does.

In Table 3, all three parameters were classified as high risk because they exceed the acceptable minimum level (0.3) for many days; it can even reach more than 0.8. The typical classification is generally daily, as the curves precisely shows (see Figure 2), while Table 3 gives a general decision that encompasses the whole year. It is well known that the hazards of smelting furnaces are very sensitive to the fear of explosion resulting from high pressure levels or high temperatures, while for low temperatures, liquid iron can freeze inside the furnace.

Figures 2 shows upper/lower risks of each variable followed by the combined risk from both upper and lower limits simultaneously, respectively. It is noteworthy that all variables exceed the control limit. For instance, the pig iron temperature risk exceeds more than 15 times, Circular pressure risk

surpasses it more than 22 times, and Hot wind temperature risk exceeds it more than 13 times.

Figure 3. displays global multiplicative/additive risks. For the additive risk, every day carries a significant level of risk, whereas the system indicate only two warnings related to the multiplicative risk.

Figure 4. and Table 4. show the results for the regression analysis in two parts modeling and prediction using different developed methods such as RBANN and ESRBANN. These obtained results show effective multivariate techniques, used to treat complex data sets, as described in Sections 3.3. and 3.4. In addition, the proposed method ES-RBANN provides the highest prediction accuracy when compared to the conventional RBANN approaches and can be considered as the best tool. In the modeling part, 294 samples are used for training, while a new data set of 71 samples are used for testing.

For RBANN approach, two hidden layers were used, where in the first one the activation function was the radial basis transfer function (Radbas) with 20 neurones, while in the second, the symmetric sigmoid transfer function (tansig) was used as an activation function with 10 neurones. The number of learning epochs was set to 500, and the used algorithm was the one due to Levenberg Marquardt. However, in the case of ES-RBANN technique, the parameter alpha was set to 0.001. The performance function used here is the “Mean squared normalized error”.

Figure 5. shows the regression function. Here the coefficient of determination R-squared = 0.9476 is very high, indicating that the regression model using neural networks is performing very well. This implies that the independent variables in the model indicate about 94.76% of the variance in the dependent variable. In simple terms, the model captures and predicts the relationships between the features and the target variable well.

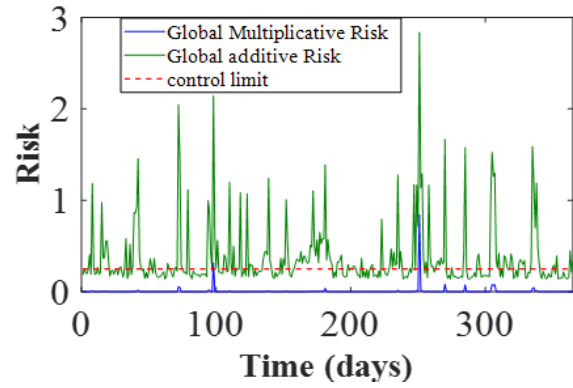


Fig. 3. Global Risks additive and multiplicative

Table 3. Conformity and Nonconformity decision

Risks	Decision	Risk level
Pig iron temperature	Nonconformity	high risk
Circular pressure	Nonconformity	high risk
Hot wind temperature	Nonconformity	high risk

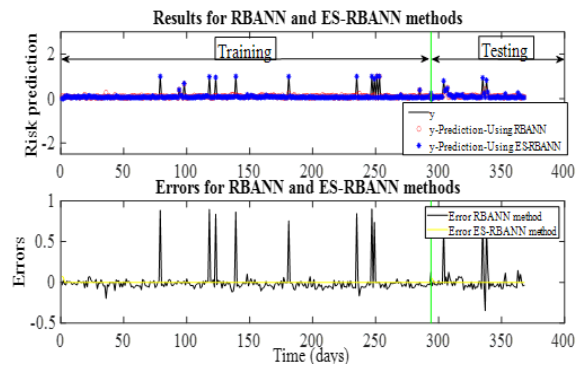


Fig. 4. Training and testing of pig iron temperature risk prediction and Errors

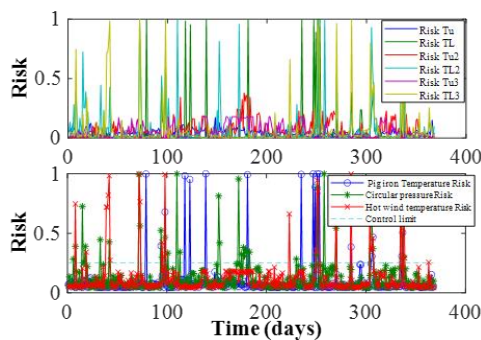


Fig. 2. Risks of different parameters

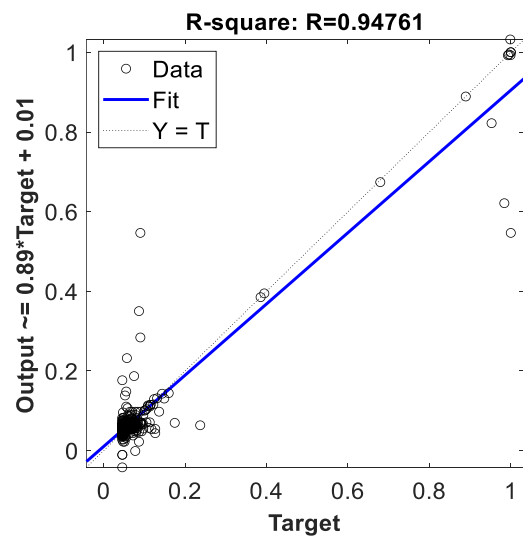


Fig. 5. Regression function

Table 4. Statistical performance indicators of RBANN and ES-RBANN methods

Methods	STD (Training)	STD (Testing)
RBANN	0.0828	1.2477
ES-RBANN	0.0056	0.0085

Table 5. Coefficients

Coefficients 1	Coefficients 2
-7.6646	14.1245
-5.4007	-3.6715
1.6611	0.3191
-2.4965	-5.6045
-6.3913	5.6646
12.4783	-9.8946
2.6868	5.9346
-0.4034	8.0453
9.9743	5.5347
-6.5638	-1.8671
4.9285	-26.8890
5.6585	-4.7716
-2.9955	19.4189
7.5337	-14.6419
-7.3624	6.3862
-20.9519	17.0846
-3.1086	33.3460
6.2603	-6.8819
18.0804	-12.7824
-5.3086	-3.5737
-0.1424	15.1360
-0.1424	15.1360
-0.3409	-6.3014
-39.1578	43.4974
-4.6247	6.0376
-4.8445	2.2710

5. CONCLUSION

This work is a modest contribution to the field of control systems, focusing on strengthening the critical task of risk detection and mitigation. This vital task is inextricably linked to the improvement of safety protocols and the minimization of system failures. Our principal findings are:

(1) We have successfully carried out a comprehensive multivariate risk assessment, combined with an in-depth examination of failure systems, using a combination of statistical distribution models, including the normal distribution, and advanced machine learning methodologies,

(2) The obtained results clearly underscore the superior precision and accuracy of the ES-RBANN technique compared to the conventional RBANN method, particularly in handling uncertainties and risk quantification,

(3) Our generated models have gone through extensive validation procedures using real-world data, confirming their practical applicability and value.

Acknowledgement: *The authors are extremely appreciative to ArcelorMittal Annaba Algeria for*

supplying the reliable data necessary to complete this modest work.

Source of funding: *This research received no external funding.*

Author contributions: *research concept and design, A.A., S.B.; Collection and/or assembly of data, S.B.; Data analysis and interpretation, A.A.; Writing the article, A.A.; Critical revision of the article, A.A., F.Z.N., S.B.; Final approval of the article, F.Z.N., S.B..*

Declaration of competing interest: *The authors declare that they have no known competing financial interests or personal relationships that could have appeared to influence the work reported in this paper.*

REFERENCES

- Abdelaziz M, Ahmed A, Riad A, Abderrezak G, Djida AA. Forecasting daily confirmed COVID-19 cases in Algeria using ARIMA models. 2020; 2020.12.18. 20248340. <https://doi.org/10.1101/2020.12.18.20248340>.
- Alam MA, Emura K, Farnham C, Yuan J. Best-Fit Probability Distributions and Return Periods for Maximum Monthly Rainfall in Bangladesh. *Climate* 2018; 6(1): 9. <https://doi.org/10.3390/cli6010009>.
- Bttinger D, Fritschek H, Kronberger T, Mauhart J, Schaler M. Risk and Knowledge Management With Blast Furnace Process Optimization Systems. *IRON & STEEL TECHNOLOGY* 2018.
- BIPM, IEC, IFCC, ILAC, ISO, IUPAC, IUPAP and OIML, Joint Committee for Guides in Metrology - JCGM 106:2012, Evaluation of Measurement Data - The Role of Measurement Uncertainty in Conformity Assessment (2012).
- Clemen RT, Winkler RL. Combining Probability Distributions From Experts in Risk Analysis. *Risk Analysis* 1999; 19(2): 187–203. <https://doi.org/10.1111/j.1539-6924.1999.tb00399.x>.
- Faris H, Aljarah I, Mirjalili S. Chapter 28 - Evolving Radial Basis Function Networks Using Moth-Flame Optimizer. *Handbook of Neural Computation* 2017 s. 537–50. <https://doi.org/10.1016/B978-0-12-811318-9.00028-4>.
- Gao X, Zhou X, Zou H, Wang Q, Zhou Z, Chen R, i in. Exposure characterization and risk assessment of ultrafine particles from the blast furnace process in a steelmaking plant. *Journal of Occupational Health* 2021; 63(1): e12257. <https://doi.org/10.1002/1348-9585.12257>.
- Ge Z, Song Z, Ding S, Huang B, Data mining and analytics in the process industry: The role of machine learning. *IEEE Access* 20590-20616 2017. <https://doi.org/10.1109/ACCESS.2017.2756872>.
- Kamo K, Hamamoto K, Narazaki H, Maeda T, Yakeya M, Tanaka Y. Method for predicting gas channeling in blast furnace. *Kobelco Technology Review* 2019; 37: 41-47.
- Kara Y, Canal MR, Sefa İ, Boran FE. Selecting and Analyzing Appropriate Probability Distributions for Reliability of Electrical Transmission Lines. *Gazi University Journal of Science Part C: Design and Technology* 2021; 9(1): 108–21. <https://doi.org/10.29109/gujsc.868923.11>.
- Li, Junpeng and Hua, Changchun and Yang, Yana and Guan, Xinping. "Data-driven Bayesian-based takagi-

sugeno fuzzy modeling for dynamic prediction of hot metal silicon content in blast furnace". IEEE Transactions on Systems, Man, and Cybernetics: Systems, 2020.

- <https://doi.org/10.1109/TSMC.2020.3013972>
12. Liu S, Sun W. Attention mechanism-aided data and knowledge-driven soft sensors for predicting blast furnace gas generation. *Energy* 2023; 262: 125498. <https://doi.org/10.1016/j.energy.2022.125498>.
 13. Luo Z, Chen L, Zhang M, Liu L, Zhao J, Mu Y. Analysis of melting reconstruction treatment and cement solidification on ultra-risk municipal solid waste incinerator fly ash–blast furnace slag mixtures. *Environmental Science and Pollution Research* 2020; 27(25): 32139–51. <https://doi.org/10.1007/s11356-020-09395-8>.
 14. Modarres M, Kaminskiy MP, Krivtsov V. Reliability engineering and risk analysis: a practical guide. CRC press 2017. <https://doi.org/10.1201/9781315382425>.
 15. Richardson JW, Klose SL, Gray AW. An Applied Procedure for Estimating and Simulating Multivariate Empirical (MVE) Probability Distributions In Farm-Level Risk Assessment and Policy Analysis. *Journal of Agricultural and Applied Economics* 2000; 32(2): 299–315. <https://doi.org/10.1017/S107407080002037X>.
 16. Sun W, Wang Z, Wang Q. Hybrid event, mechanism and data-driven prediction of blast furnace gas generation. *Energy* 2020; 199: 117497. <https://doi.org/10.1016/j.energy.2020.117497>.
 17. Suresh, R and Sathyanathan, M and Visagavel, K and Rajesh Kumar, M, Risk assessment for blast furnace using FMEA. *Int J Res Eng Technol* 2014; 3.
 18. Xie T, Yu H, Wilamowski B. Comparison between traditional neural networks and radial basis function networks. 2011 IEEE International Symposium on Industrial Electronics 2011; 1194–9. <https://doi.org/10.1109/ISIE.2011.5984328>.
 19. Zhang X, Kano M, Matsuzaki S. Ensemble pattern trees for predicting hot metal temperature in blast furnace. *Computers & Chemical Engineering* 2019; 121: 442–9. <https://doi.org/10.1016/j.compchemeng.2018.10.022>.
 20. Tang X, Zhuang L, Jiang C. Prediction of silicon content in hot metal using support vector regression based on chaos particle swarm optimization. *Expert Systems with Applications* 2009; 36(9): 11853–7. <https://doi.org/10.1016/j.eswa.2009.04.015>.



Abdelhakim AZZEDINE

is a Phd Student in the Mathematical Modelling and Numerical Simulation Research Laboratory. He taught tutorials on numerical methods and probability and statistics.

He obtained a Bsc degree in Mathematics in 2014 and a Master in 2017 in Differential Equations and Scientific

Computing from BadjiMokhtar university, Annaba-Algeria.

His research interest include Mathematical Modelling, Mathematical Analysis, Numerical Methods, Artificial intelligence, Database Analysis.

Email address: azzedine.abdelhakim@gmail.com



Fatma Zohra NOURI

is a full professor at the Badji Mokhtar University, Annaba-Algeria (UBMA).

She obtained a Bsc. Honors in Mathematics Functional Analysis in June 1983 from the university of Annaba-Algeria and awarded a Grant for Postgraduate Studies in England, where she obtained a Msc. in October 1985 in

Modeling and Numerical Analysis, then a Phd in Nov. 1988 in Applied Mathematics from Oxford-Strathclyde universities-UK.

She has been the Dean of the Faculty of Sciences 2000-2003 and the director of Mathematical Modelling and Numerical Simulation Research Laboratory, from Jan.2012-Feb.2023. She is the Vice President of the Algerian Society of Applied Mathematics.

She has contributed as a member of the Ethics and Deontology Committee in UBMA, since 2020;

as a member of Finance and Dues Committee 2020-2022 in the International Mathematical Union and since July 2022 as a member of Resolutions Committee.

She is a member of Mathematics in Medicine and Qualitative Systems in Pharmacology UK-Study Groups, since 2009 and received a Life time Achievement Award, International Scientist Awards 2020 in Engineering, Sciences and Medicine.

Her Research Interests are Differential Equations, Modeling & Numerical Analysis, Spectral Methods, Algorithmic and Code developments, Methods for Image processing, Mathematics in Industry, Medical Sciences and Science of Plants.

Email address: tassili.nan09@gmail.com



Dr. Salah BOUHOUCHE is a Senior Researcher/Directeur at his own R&D, Innovation and consulting Bureau as a scientific and technological support for companies, since 2021.

He obtained a diploma in Engineering, option "Control and instrumentation", in 1985 from the Algerian Institute of Hydrocarbons and Chemistry,

Boumerdes, Algeria, and an MPhil degree in 1995, in Control Engineering from the Algerian National Polytechnic School, Algiers-Algeria.

From 1996, he contributed in the field of the Mathematical Modeling and Simulation in Steel Industry and obtained a PhD in 2002, in Mechanical Engineering/Controlled Solidification in Continuous Casting from Freiberg Mining and Technical University (TU Bergakademie) Germany.

He obtained a State Doctorate Degree, in Control Engineering from the Algerian National Polytechnic School

He worked as a research engineer at the Applied Research Unit in the Algerian steel industry, (DRA-SIDER Group, Spa), from 1988 to 1991. He was the director of Applied Research Unit in Steel and Metallurgy from 2013-2018, Annaba

He worked for more than thirty years between R&D in Industry and Academic.

His field of interest is Mathematical Modeling of Complex Real Chemical, Mechanical and Electrical industrial systems.

Email address: bouhouche11@yahoo.fr